

The Characteristics of Rim-Driven Propulsor's Flow Field

Chung-Wei Lee

Department of Systems and Naval Mechatronic Engineering,
National Cheng Kung University
1 University Rd., Tainan 70101, Taiwan
1104tom@yahoo.com.tw

Jeng-Horng Chen

Department of Systems and Naval Mechatronic Engineering,
National Cheng Kung University
1 University Rd., Tainan 70101, Taiwan
chenjh@mail.ncku.edu.tw

ABSTRACT

Rim-driven propulsor as a new type of propulsor which has been already applied on underwater vehicles and bow thruster of ships has not been systematically studied. The present research use a phase-locked PIV system to measure velocity fields of three types of propulsors in NCKU's cavitation tunnel. These three types of propulsors include a traditional propeller, a rim-driven propeller with hub, and a hubless rim-driven propeller. They are designed to the same thrust and similar dimensions. Results show that the rim-driven propellers have much weaker tip vortices and root vortices. The hub vortex and turbulence intensity of rim-driven propeller with hub is also smaller than that of traditional propeller. Rim-driven propellers also have more uniform wake than traditional propeller..

INTRODUCTION

Rim-driven propeller has been invented for several years when brushless permanent magnet motor technology became mature, and has been applied on underwater remotely operated vehicle (ROV) (e.g. Alstom Schilling's Quest ROV, as seen in Fig.1) and bow thrusters on surface ships (e.g. Van Der Velden's EPS thruster). Rim-driven propulsors with the possibility of not needing a centre hub as bearing may lead to some significant characteristics in flow field, mechanism and performance. Thus, this type of propulsor has great potential for unconventional propulsor, turbine, or pump design. However, there has been almost none academic research on this new type of propulsor yet, even though commercial products are already available.

Therefore, for possible future improvement of this new type of propulsor, the purpose of this research is to investigate the characteristics of the turbulent flow field generated by the rim-driven propulsor. With the disappearing of a centre hub, rim-driven propulsor's blades may have their tips near the centre of rotation. This leads to a possible much weaker tip vortex phenomena. Cavitation and turbulence problems caused by hub vortex, root vortices, and tip vortices as seen in traditional propellers may be highly reduced in rim-driven propulsors. Hence, a much quieter propulsor is possible.

Most of past propeller researches used multi-hole Pitot tubes or LDV (Stella et al., 2000) for single point statistical measurement. Recent use of Particle Image Velocimetry (PIV) on single traditional propeller researches (Cotroni et al., 2000; Calgani et al., 2002; Scarano et al., 2002; Lee et al., 2002; Paik et al., 2004) captured propeller's instantaneous flow field structure well with a price of slightly more difficult experimental set-up. The present research used similar PIV technique to study and compare the turbulent flow fields of three kinds of propulsors with similar dimension and performance: a rim-driven hubless propulsor, a rim-driven propulsor with hub, and a traditional single propeller.

EXPERIMENTAL METHODS

Propeller Design

Even though there is no appropriate theoretical work for designing a hubless propeller, three types of propeller used in this research were preliminarily designed using a computer code based on lifting line theory. Lifting line theory has been proved to be a useful preliminary design tool for traditional propellers. Its error is within acceptable region and could be improved by lifting surface theory. With no suitable design tool for hubless propellers, the present research still used lifting line code to design it and the design result could be checked after experimental test.

The design condition for three types of propulsors is the same: to match a 49N thrust at 3m/s inflow speed and 1500rpm of rotational speed, as for a typical small size remotely-operated underwater vehicle. The diameter of propeller blade was set to 100mm. The outer diameter of duct of rim-driven propulsor was limited to 160mm for accommodating driven mechanism and considering the test section size and wall effect. Propellers were driven by a 0.5hp motor at 1500rpm. The inflow velocities measured were 1.8m/s, 2.4m/s and 3.0m/s for all propellers. All three kinds of propellers had five blades. Hence, measurements were taken at 0°, 18°, and 36° phase angles. The blade geometries of three propellers were optimized (best circulation distribution) for obtaining the best efficiency. They are all installed at the end of a cylinder that could be

viewed as the rotational part on a real POD propulsor. The geometries of traditional and rim-driven propellers and the driven mechanism are shown in Fig.2 and Fig.3, respectively. Their sizes and performances are similar, so the comparison of their flow fields is meaningful.

It should be noted that the maximum designed efficiencies of these propellers are not the same. The efficiency of traditional propeller, rim-driven propeller with hub, and hubless rim-driven propeller are about 50%, 46% and 37%, respectively. The reason that they are not the same is that the maximum efficiency for rim-driven propellers occur at a lower rotational speed, while it is required that they are compared using the same motor at a higher rotational speed. It will be necessary to study their difference when they can be designed to their best efficiency in the future.

Apparatus and Instruments

PIV measurements of these propulsors' flow fields were conducted in a closed-loop vertical water tunnel with test section of 0.3m(H)x0.3m(W)x1.2m(L). The turbulence intensity of the tunnel is quite uniform and less than 1.1%. Titanium dioxide (TiO₂) particles (TSI model 10086A) were used as tracing particles. A dual pulse Nd:YAG laser (Quantel Twins, 0.15J/pulse, 10Hz repeating rate) and optical lenses (TSI model 610090, 610092, 610094) generated a laser sheet for a CCD camera (TSI Model 630046 PIVCAM 10-30, 1008x1024 pixels). A dual-processor personal computer with a frame grabber (TSI Model 600067) was used to capture, store and analyse images using TSI Insight 5.0 software. A synchronizer (TSI Model 610034) synchronized all instruments. A 45-degree mirror was installed far downstream for cross-streamwise velocity measurement. All apparatus are shown in Fig.4.

Images were taken at three fixed phases of propeller's motion. Therefore, a fiber-optic sensor (Keyence FS-V11) was used to detect the motor's rotation and trigger PIV system at the same phase. Both streamwise and cross-streamwise velocities were measured 100mm (one time of propeller diameter) downstream of propellers as seen in Fig.5. Streamwise velocities were measured in a 70mmx70mm square area and cross-streamwise velocities were in a 130mmx130mm square area. Direct measurement errors due to image distortion, background turbulent flow and image processing all together were less than 1.5%.

RESULTS AND DISCUSSION

The PIV results of traditional propeller and hubless rim-driven propulsor show the following characteristics. First, cross-streamwise velocities of traditional propeller are much faster than both rim-driven propellers as seen in Fig. 6, which shows typical results at 3m/s inflow speed and 18° phase angle. Both rim-driven propellers' wakes have a slight downward tendency, which is probably due to the attraction of the wake of the POD's cylinder connecting the duct and the wall of test section. It is also clear that both rim-driven propellers' root vortices are not strong such that it is not easy to identify them. This is probably due to a different vortex sheet system of hubless rim-driven propeller because its blade geometry is designed to share

circulation distribution in radial direction more averagely than conventional one.

Second, the turbulence intensity distribution of rim-driven propeller's wake is more homogeneous and weaker than traditional one, as seen in Fig. 7. The hub vortex and tip vortices of traditional propeller are very strong and clear. They contribute to most of the turbulence in traditional propeller's wake. But the rim-driven propeller with hub also has an obvious centre region with a higher turbulence intensity due to its hub vortex. On the other hand, the hubless rim-driven propeller's turbulence intensity is very homogeneous inside the duct. The wake of thick duct of rim-driven propulsor caused a strong turbulent wake outside the blade wake. It contributes the most part of turbulent flow. Notice that the present duct was neither designed to have a streamline shape, nor accelerate/decelerate velocities. Instead, it was designed merely to cover the driven mechanism, and did not generate any thrust. Nevertheless, the strong turbulence caused by strong tip vortices and hub vortex of traditional propeller as seen in Fig. 7 disappear in hubless rim-driven hubless propulsor cases.

Third, the vorticity fields of three propellers shown in Fig.8 also demonstrate the same trend. Traditional propeller's strong hub vortex and tip vortices are obvious. On the other hand, hubless rim-driven propulsors' tip vortices locating near the center are much weaker. This is reasonable because the tangential velocity of blade tips of rim-driven propulsor is smaller than that of traditional propeller due to its smaller radius. Moreover, its root vortices with similar strength but different direction are also clearly seen. The hubless rim-driven propeller has stronger root vortices than tip vortices. This is opposite to traditional one because its tips are inside now and thus have smaller tangential velocities and tip vortices. This is also the reason that it may be able to reduce tip vortices and potential cavitation/noise problem. A rim-driven propulsor may be also designed to have their tips contacting each other at the center ($r=0$) with the same pitch angle of 90 degree. This new design shall be studied in the future to explore any potential uses.

Besides, both turbulence intensity and vorticity distribution show that there exists a small area at the centre (near $r=0$) not affected by blade motion of hubless rim-driven propeller. The flow is neither accelerated by propulsor nor rotating. The inflow just flows through this region with almost no change. In another word, the tip vortices are not strong and large enough to affect this centre region.

This special characteristic was already expected during lifting line theoretical design. It also implies that a rim-driven propeller may be able to extend its blade to the centre of rotation to have more area providing thrust, or to deliberately leave this gap for more animal friendly consideration, or to pursue a propeller with lower possibility of tangling, because this centre gap together with the lack of bearing structure will largely decrease the complexity of structures within the duct and thus decreases the possibility of soft tissue or net tangling problem. These objectives may be emphasized in future turbine and pump design. Of course, more studies will be needed to verify these potential advantages.

CONCLUSIONS

PIV measurements of the wakes of three types of propellers (traditional propeller, rim-driven propeller with hub, and hubless rim-driven propeller) were conducted in a water tunnel. The results show that rim-driven propellers have more uniform wakes, less turbulent wakes, and smaller vorticity fields than traditional one. The hubless rim-driven propeller has stronger root vortices than tip vortices. Its turbulence intensity and wake are both slightly more uniform than rim-driven propeller with hub. The hubless rim-driven propeller also has a center region with no disturbance of blade motion. These characteristics may imply that a hubless rim-driven propeller is more animal-friendly, much quieter, less possible to have cavitation, and harder to trace.

ACKNOWLEDGEMENT

This research was supported by ROC's National Science Council, project No. NSC 95-2611-E-006-003- and NSC 95-2611-E-006-005-.

REFERENCES

Calcagno, G.; Di Felice, F.; Felli, M.; Pereira, F., 2002, "Propeller Wake Analysis Behind a Ship by Stereo PIV", Twenty-Fourth Symposium on Naval Hydrodynamics, Fukuoka, JAPAN, 8-13 July 2002.

Cotroni, A.; Di Felice, F.; Romano, G. P.; and Elefante, M., 2000, "Investigation of the near Wake of a Propeller Using Particle Image Velocimetry", Experiments in Fluids S227-S236.

Lee, S.J.; Paik, B.G.; and Lee, C.M., 2002, "Phase-Averaged PTV Measurements of Propeller Wake", Twenty-Fourth Symposium on Naval Hydrodynamics, Fukuoka, JAPAN, 8-13 July 2002.

Paik, B.G.; Lee, C.M.; Lee, S.J., 2004, "PIV Analysis of Flow Around a Container Ship Model with a rotating Propeller", Experiments in Fluids, Vol.36, pp.833~846.

Scarano, F.; van Wijk, C.; and Veldhuis, L.L.M., 2002, "Traversing Field of View and AR-PIV for Mid-field Wake Vortex Investigation in a Towing Tank", Experiments in Fluids, Vol.33, pp.950~961.

Stella, A.; Guj, G.; & Di Felice, F., 2000, "Propeller Wake Flowfield Analysis by Means of LDV Phase Sampling Techniques", Experiments in Fluids, Vol.28 , pp.1-10.

Tsuei, L.; Savas, O., 2000, "Treatment of Interfaces in Particle Image Velocimetry", Experiments in Fluids, Vol.29, pp.203-214.

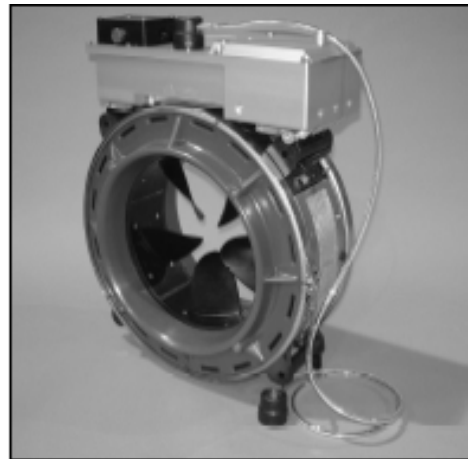


Fig.1 A rim-driven propulsor on a remotely-operated vehicle (ROV) produced by Alstom.

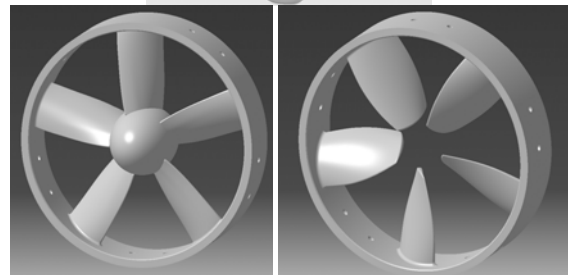
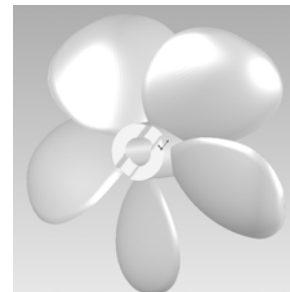


Fig. 2 Traditional propeller, rim-driven propeller with hub, and hubless rim-driven propeller

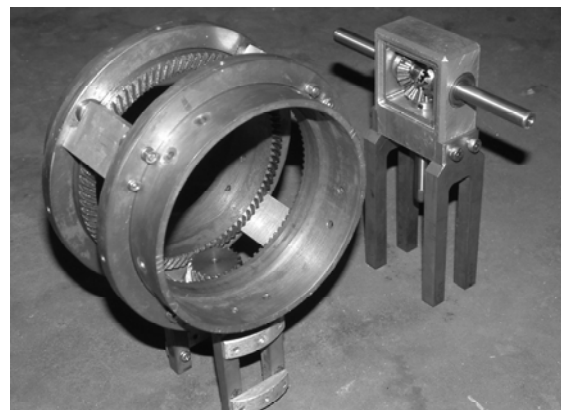
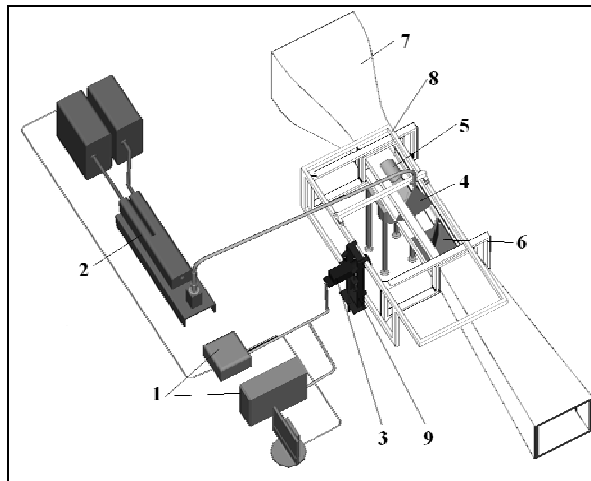


Fig.3 The driven mechanisms for rim-driven propellers (left) and traditional propeller (right)



- | | |
|----------------------|----------------------|
| 1. PC&Synchronizer | 6. Reflecting Mirror |
| 2. Nd:YAG Laser | 7. Cavitation Tunnel |
| 3. PIV Camera | 8. Observation Track |
| 4. Laser Light Sheet | 9. Camera Track |
| 5. POD of Propeller | |

Fig.4 Experimental Set-up

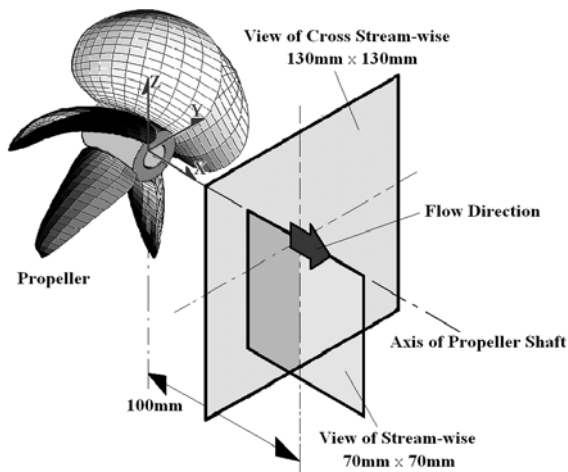
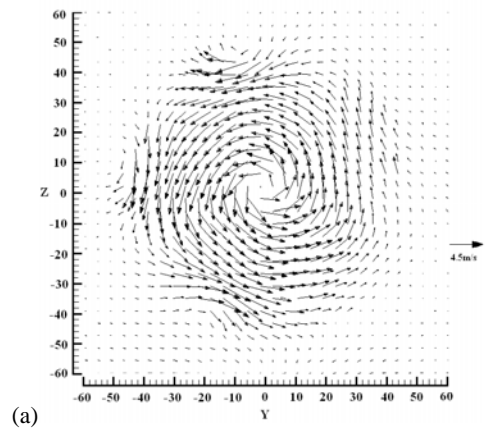
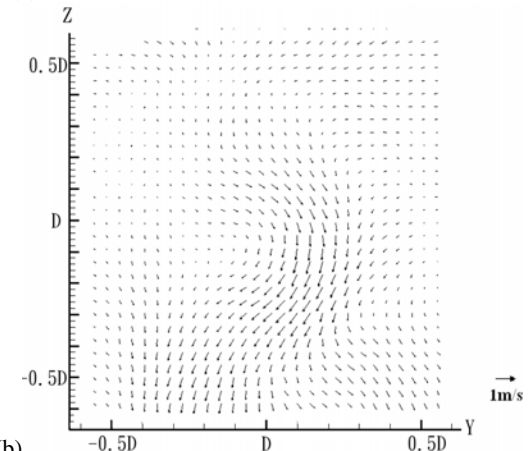


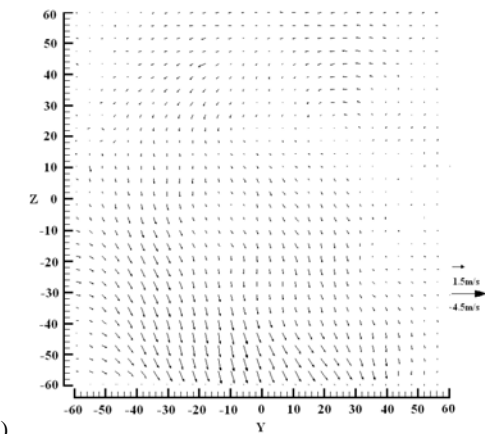
Fig.5 Investigated flow field orientation



(a)



(b)



(c)

Fig.6 Cross-streamwise velocities of (a) traditional propeller, (b) rim-driven propeller with hub, and (c) hubless rim-driven propeller at 3m/s inflow and 18° phase angle.

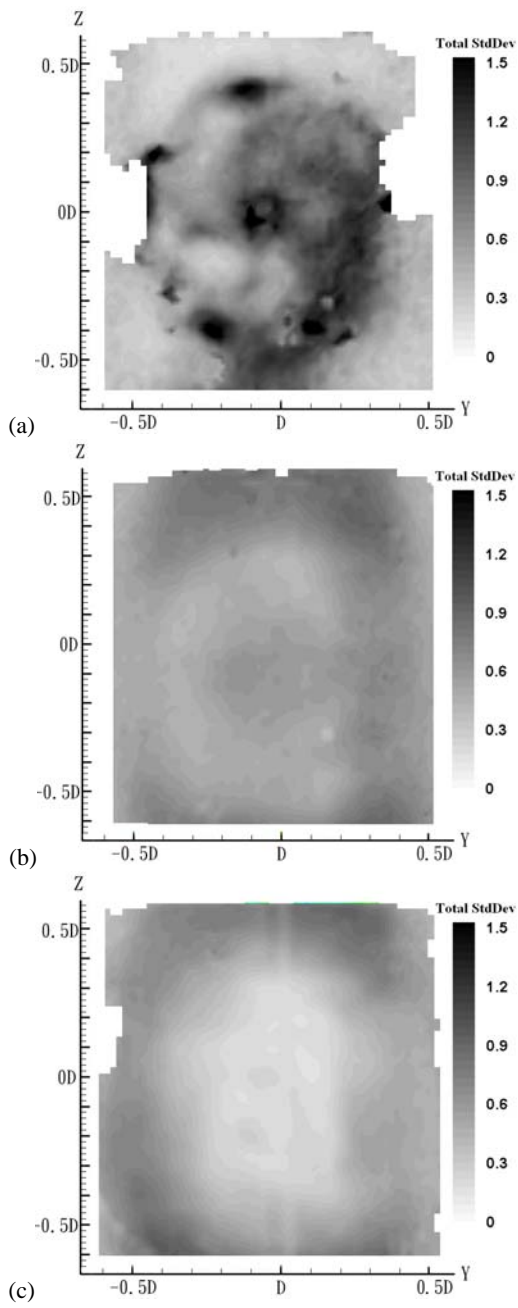


Fig.7 Turbulence intensities of (a) traditional propeller, (b) rim-driven propeller with hub, and (c) hubless rim-driven propeller at 3m/s inflow and 18° phase angle.

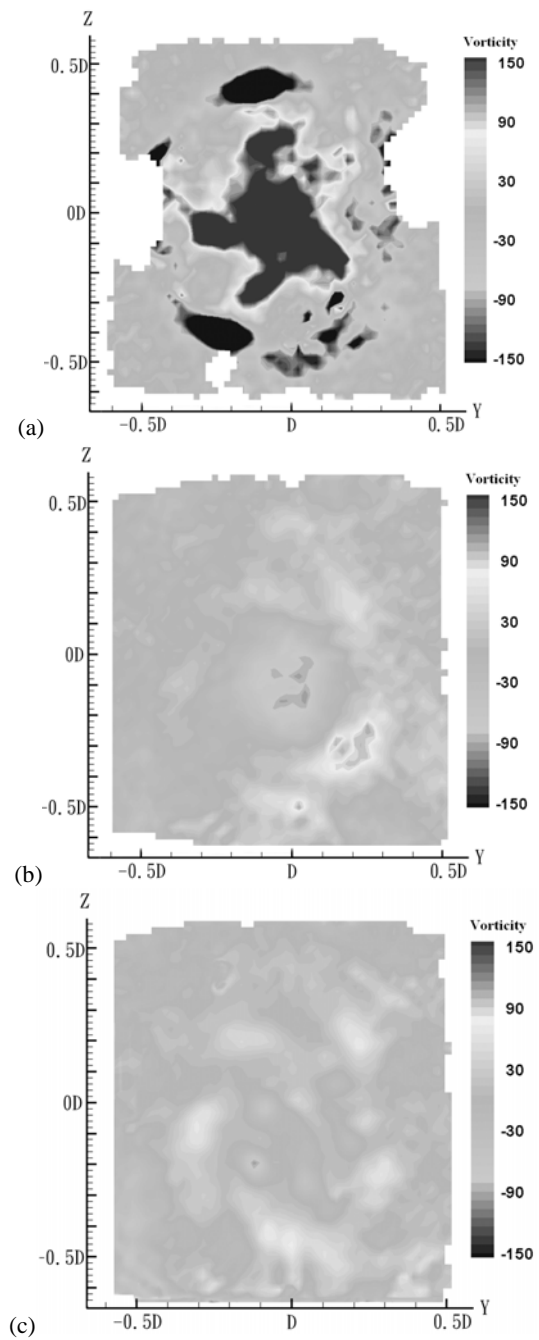


Fig.8 Vorticity fields of (a) traditional propeller, (b) rim-driven propeller with hub, and (c) hubless rim-driven propeller at 3m/s inflow and 18° phase angle.